



# Development of environmentally friendly inkjet printable carbon nanotube-based conductive ink for flexible sensors: effects of concentration and functionalization

John O. Akindoyo<sup>1</sup>, Nurul Hidayah Ismail<sup>1</sup>, and M. Mariatti<sup>1,\*</sup> 

<sup>1</sup> School of Materials and Mineral Resources Engineering, Universiti Sains Malaysia, Engineering Campus, 14300 Nibong Tebal, Pulau Pinang, Malaysia

**Received:** 25 November 2020

**Accepted:** 2 April 2021

**Published online:**  
20 April 2021

© The Author(s), under exclusive licence to Springer Science+Business Media, LLC, part of Springer Nature 2021

## ABSTRACT

The fabrication of environmentally friendly printed flexible sensors is still an emerging technology, but with vast potential applications. Among the available printing techniques, inkjet printing is considered as a promising technique for flexible electronics because it enables high volume and versatile manufacturing, at low environmental impact. This study demonstrates a simple and facile method of preparing an environmentally benign water-based conductive ink, by dispersing functionalized and non-functionalized multi-walled carbon nanotubes (MWCNTs) in aqueous solution with the help of a biopolymer surfactant. The concentration of CNTs in the ink formulation was varied from 0.25 to 0.75 wt%, and additives such as triton-x 100, polypropylene glycol, and defoamer were added to achieve desirable ink properties. Inkjet printable ink was produced, and it was observed that the conductivity of the printed pattern is dependent on the printing pass. In addition, it was found that as the number of printing layer increases, there is higher synergy between concentration and number of printing pass in F-MWCNTs printed ink to produce higher electrical conductivity, compared to MWCNTs printed ink. Generally, the findings of this study could potentially open opportunities for global economic growth through the applications of printed, low cost and environmentally friendly flexible sensors.

Address correspondence to E-mail: mariatti@usm.my

## 1 Introduction

In recent years, there has been a significant interest in the development of printed flexible electronics. This technology is growing rapidly and it is envisaged that the market for printed flexible electronics would reach \$8.5 billion by 2029 [1]. This will undoubtedly enhance global economic growth. This is partly because of the vast potential application of this technology in different sectors including energy storage [2], touch screens [3], electronic textiles [4] sensors [5, 6], food security [7], radio frequency tags [8], electronic paper [9], and health diagnostics [10]. One of the notable processes involved in the fabrication of flexible printed electronics is the production of conductive inks. The conductive ink industry has been greeted with an unprecedented bloom in the past few years [11]. Two kinds of materials such as noble metal based (copper and silver) [12], and carbon based (CNTs and graphite) [13] are commonly used for conductive inks and each of these class of materials present peculiar advantages and disadvantages. Generally, the wide application of printable metals in printed electronics is mainly limited by their exorbitant prices (like the case of Ag, Au, and Pt), or poor oxidation properties (as in the case of Cu). However, carbon nanotubes (CNTs) is considered as a promising material for printed electronics.

Carbon nanotubes (CNTs) have been extensively investigated as a potential candidate for nanoelectronics and optoelectronic applications. This is based on its exceptional physical, mechanical, and electrical properties, compared to conventional conductive materials [14]. For instance, unlike Indium tin oxide (ITO), which may crack with bending, CNTs offer more reliable option for the fabrication of flexible sensors [15]. Therefore, different printing techniques have been developed over the years to integrate the unique properties of CNTs onto flexible substrate materials. The common CNT printing techniques include inkjet printing, screen printing, aerosol printing, transfer printing, and contact printing. Among these printing techniques, inkjet printing (IJP) has become one of the most desirable methods for the fabrication of flexible and wearable printed electronics [16]. Particularly, the IJP technology is promising in the field of printed sensors because it is an entirely digital technique. Hence, print designs can be easily altered with little or no additional cost implication [17, 18]. This makes IJP technique highly

attractive to the production environments, and it is equally suitable for research and prototyping purposes. In addition, this technique ensures minimal waste of ink, and it offers the possibility to print inks over a wide range of layer thickness and line widths, while maintaining higher edge sharpness of deposition [19]. Therefore, inkjet printing of CNTs offers a synergy where the salient features of IJP and the exceptional properties of CNTs can be exploited.

Nevertheless, the practical feasibility of IJP requires that several challenges be addressed. Specifically, recent advances in inkjet printing demands that the ink is environmentally benign, and easy to process. In addition, the ink formulation should not be time-consuming, to facilitate scalable fabrication of functional devices. Furthermore, the ink should possess suitable fluidic properties including particle dispersion, stability, viscosity, and surface tension [19]. Although single-walled carbon nanotubes (SWCNTs) [20], and multi-walled carbon nanotubes (MWCNTs) [21] can be used to produce conductive inks, the interest of this study is on MWCNTs. There are reports on the synthesis of MWCNT nanofluids by using different base fluids including water, glycerol, poly( $\alpha$ -olefin) oil (PA06), silicon oil, and ethylene glycol [21, 22]. Likewise, the effects of surfactants on the viscosity and conductivity of MWCNT nanofluids have been widely investigated [23, 24]. However, the development of environmentally friendly inkjet printable carbon nanotube-based conductive ink for sensor applications has not been fully investigated.

Therefore, in this contribution, we have developed a simple method to produce highly concentrated, stable, inkjet-printable, water-based inks by dispersing MWCNTs in water. The ink production does not involve solvent exchange, chemical treatment, or other aggressive conditions. Dispersion and stability of MWCNTs in water was achieved with the help of gum Arabic which was used as dispersant, and few other additives. The aqueous dispersion was dispensed on a polyurethane (PU) substrate using a commercial desktop inkjet printer, and the effect of MWCNT content and functionalization on the stability, viscosity, surface wettability, electrical conductivity, and morphology of MWCNT water-based inks was investigated. In addition, the effect of different printing cycles on the electrical conductivity of the printed film is reported.

## 2 Materials and methods

### 2.1 Materials

The conductive materials used in this study are multi-walled carbon nanotube (MWCNTs), and functionalized MWCNTs (F-MWCNTs). The MWCNTs, procured from USAINS Holding Berhad was produced via catalytic chemical vapour deposition (CCVD) process at the School of Chemical Engineering, Universiti Sains Malaysia. The MWCNT (> 95 % purity) has an average diameter of 10 nm and average length of 1–5  $\mu\text{m}$ . The –OH functionalized MWCNT was equally procured from USAINS Holding Berhad. The dispersant used to facilitate the dispersion of conductive particles in water is gum Arabic (GA) (El-Nasr brand) which was procured from a local supplier. Other materials used in the ink formulation are Triton-x 100 and propylene glycol which were used to reduce surface tension and to increase viscosity of the water-based inks, respectively. These two chemicals were supplied by Sigma-Aldrich. Furthermore, a silicone-based defoamer, supplied by a local supplier was used primarily as an additive to eliminate the bubbles generated, following the incorporation of triton-x 100.

### 2.2 Methods

#### 2.2.1 Ink preparation

The MWCNT and F-MWCNT based inks were prepared using deionized (DI) water as the solvent. The stepwise procedure for the ink formulation is presented in Fig. 1. To start with, different wt% such as 0.25, 0.5 and 0.75 wt% (based on preliminary studies) of the active component (MWCNT or F-MWCNT)

were added into the solvent. Then the solution was sonicated with 0.5 wt% gum Arabic (GA) for 30 min. Gum Arabic was incorporated primarily because it is an efficient dispersant for MWCNT [25]. In addition, it could help to prevent agglomeration between the MWCNTs. Subsequently, additives such as triton-x 100, propylene glycol and defoamer were added, followed by stirring for 30 min using a magnetic stirrer. At this stage sonication was not used, to avoid undesirable evaporation of the solvent [11]. Same procedure was followed for both MWCNT and F-MWCNT ink formulations (Fig. 1).

#### 2.2.2 Zeta potential analysis

Zeta ( $\zeta$ ) potential analysis was used to verify the stability of MWCNT and F-MWCNT colloidal dispersions. Specifically, this was performed by measuring the repulsive or attractive forces between particles of the active ingredients suspended in the liquid. The  $\zeta$ -potential of the samples was obtained from a ZEN3600 Zeta potential analyzer (Malvern Instruments, Worcestershire, UK). Prior to measurement, the samples were sonicated for 5 min after which analysis was performed at 25  $^{\circ}\text{C}$ .

#### 2.2.3 UV–Vis analysis

The UV–Vis spectra of the different ink formulations were obtained from a Varian Cary 50 Conc, Agilent Technologies UV–Vis spectrophotometer. This was used to support the result obtained from the  $\zeta$ -potential measurement. Briefly, the formulated ink was diluted 50 times prior to UV–Vis analysis at room temperature, and data was recorded from 250 to 600 nm.

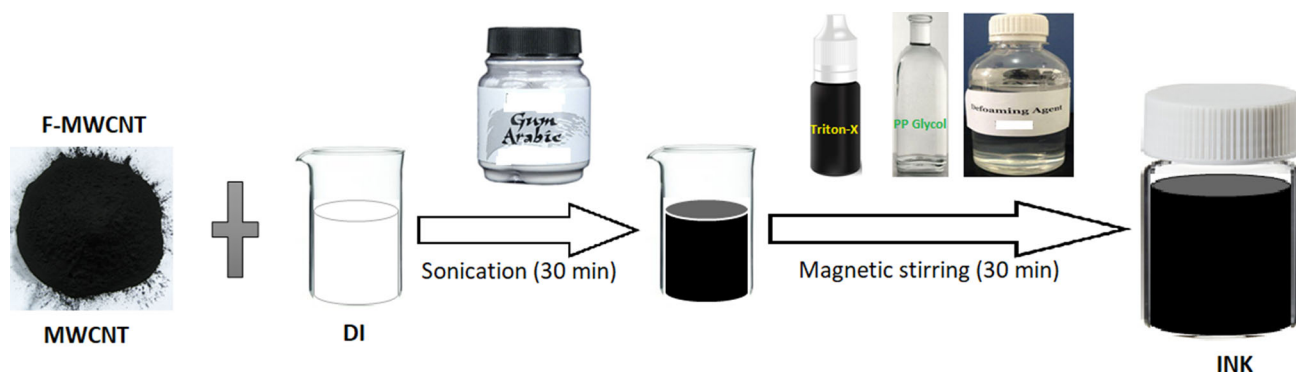


**Fig. 1** Preparation of MWCNT and F-MWCNT water-based ink

### 2.2.4 Viscosity measurement

Appropriate viscosity is needed for inkjet printing of ink. Therefore, the ink viscosity,  $\eta$ , of the different formulation was measured at a shear rate of  $50 \text{ s}^{-1}$  by a cone and plate rheometer (Physica MCR 301, Anton Paar Malaysia Sdn. Bhd.).

### 2.2.5 Contact angle measurement

Wettability of the prepared ink was investigated through contact angle measurement. The contact angle was measured by a Rame hart Instrument. Co, USA goniometer through the sessile drop. The measurement was performed using a droplet volume of  $5 \mu\text{L}$  on a PU substrate. The inks were dropped on the PU substrate and placed in a Contact Angle Goniometer which is equipped with an Image analyzer. Then, a DROPimage Advanced software was used to obtain the contact angle of the ink droplets.

### 2.2.6 Printing process

The ink was printed on a stretchable polyurethane (PU) substrate (medic transparent bandage made of PU membrane coated with a layer of acrylic adhesive) using an inkjet printer (Canon PIXMA E 510). For electrical conductivity test, six square patterns printed with 5, 10, 15, 20 and 25 passes were prepared whereas for stretching test, three dumbbell-shape patterns with 25 passes were printed. Then, the printed tracks were cured at  $70 \text{ }^\circ\text{C}$  for 30 min in an oven prior to further characterization.

### 2.2.7 Morphological analysis

The structure and morphology of the printed inks at different printing layers were observed through scanning electron microscopy. This was performed on a scanning electron microscope (SEM, FEI Quanta FEG 450, USA).

### 2.2.8 Electrical conductivity

Electrical conductivity of the printed PU was measured with a resistance meter, model Prostat-812, equipped with a miniature concentric ring fixture (PRF-912B) as depicted in Fig. 2. The miniature concentric probe was placed on the specimen as illustrated in Fig. 2. The measurements obtained using

the PRF-912B resistance fixture is approximately similar with the measurements obtained using a standard ESD Association Standard ANSI/ESD S11.11 concentric ring fixture. According to the ESD standard, to convert a resistance obtained by this method to an equivalent resistivity in ohms per square, the measured resistance is multiplied by ten. The conversion factor of ten is derived from the geometry of the electrode assembly. Six samples were tested for each ink category and the averages were recorded. Then, electrical conductivity was calculated using the following equation:

$$\sigma = \frac{1}{\rho} \quad (1)$$

where  $\sigma$  and  $\rho$  is conductivity and resistivity, respectively.

### 2.2.9 Stretching test

An INSTRON 5982 universal testing machine with a 1 kN load cell was used to perform the stretching test by generating uniaxial cyclic strains, with constant stress, strain and displacement on the printed PU. Prior to the test, the printed PU was stickled on top of the stretchable fabric bandage as depicted in Fig. 3. The fabric bandage serves as a carrier for the thin and soft PU substrate, for easy handling during stretching test. A digital multimeter (FLUKE 115) was then connected to the sensor using crocodile clips to measure the relative change in resistance as the samples were stretched.

## 3 Results and discussion

### 3.1 Particle dispersion and ink stability

Zeta ( $\zeta$ ) potential measurement is one of the reliable techniques to evaluate colloidal dispersions and ink stability [26]. The  $\zeta$ -potential values of the formulated inks containing different wt% MWCNT and F-MWCNT are illustrated in Fig. 4. Generally, the  $\zeta$ -potential value indicates the level of electrostatic repulsion between similarly charged adjacent particles of the main ingredient in the ink, whereby a high-positive magnitude ( $> +30 \text{ mV}$ ) or high negative magnitude ( $> -30 \text{ mV}$ ) of  $\zeta$ -potential indicates good stability [27]. As illustrated in Fig. 4, there is no significant difference in the  $\zeta$ -potential values of the

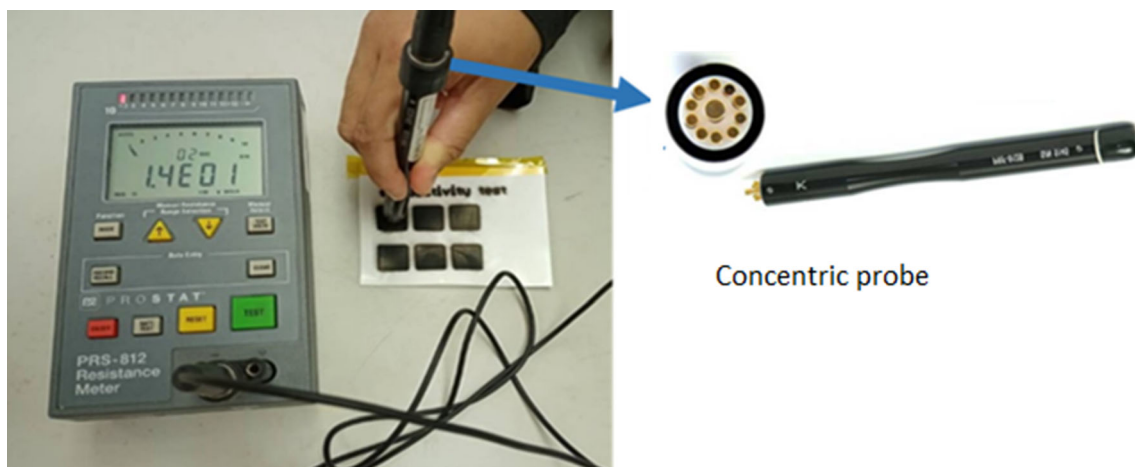


**Fig. 2** Measurement of electrical conductivity of the printed PU

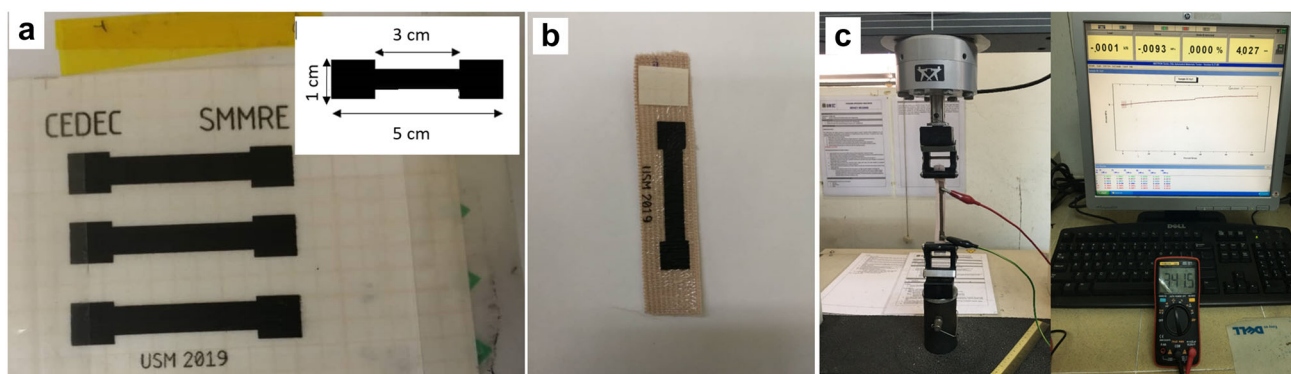


**Fig. 3** a Printed patterns on PU substrate, b printed PU is transferred onto fabric bandage, c stretching test

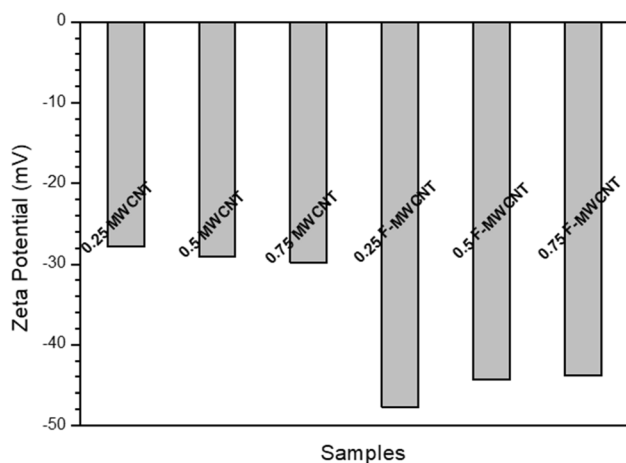


**Fig. 4** Zeta potential values of MWCNT and F-MWCNT inks at different concentration such as 0.25 wt%, 0.5 wt%, and 0.75 wt%

MWCNT inks, regardless of the MWCNT concentration. However, it is worthy of note that the  $\zeta$ -potential value of the MWCNT inks is close to  $-30$  mV

which indicates that the inks are relatively stable. This can be attributed to the presence of GA surfactant which is believed to have caused steric stabilization effect on the dispersed MWCNTs, as previously reported for graphene based conductive ink [28].

Non-ionic surfactants like GA are known to possess a hydrophilic head and hydrophobic tail. Whereas the hydrophobic tail can be easily adsorbed onto the MWCNT surface, the hydrophilic segments could extend into water such that a potential barrier is formed between the nanotubes as illustrated in Fig. 5. This might have contributed to the higher negative magnitude of  $\zeta$ -potential values ( $> -30$  mV) of the F-MWCNT inks compared to the MWCNT inks. The presence of additional functional groups on the F-MWCNTs could help to facilitate its dispersion in water. This will invariably improve the interaction between the F-MWCNTs and the GA surfactant by creating larger surface area for GA adsorption, as

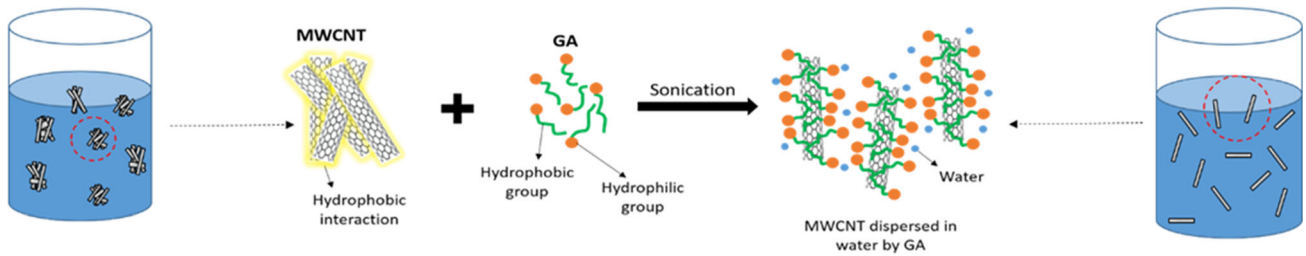


**Fig. 5** Possible mechanism of GA stabilization effect for the dispersion of MWCNTs in water

illustrated in Fig. 5. Therefore, the F-MWCNT particles would remain suspended and dispersed in the solvent.

### 3.2 UV–Vis spectroscopic analysis

In addition to  $\zeta$ -potential analysis, UV–Vis analysis was further used to investigate the particle dispersion, and stability of the formulated inks. Generally, the UV–Vis spectroscopy measures the stability of suspended particles by comparing the number of individual particles in the aqueous suspension, through their light absorbance. In the case of CNTs, only individual particles are absorptive in the UV–Vis region. On the contrary, particles that are bundled together are generally inactive within this range [29, 30]. Hence, the concentration of individually dispersed particles in the suspension would dictate the light absorbance values. The UV–Vis spectra of the MWCNT and F-MWCNT inks at different MWCNT and F-MWCNT concentrations are illustrated in Fig. 6.

It is evident in Fig. 6 that the maximum absorption is in the range of 250–270 nm for all the ink

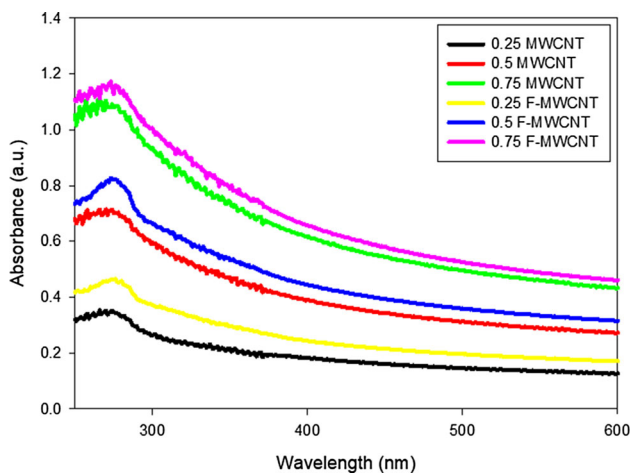


**Fig. 6** UV–Vis spectra of MWCNT and F-MWCNT inks

formulations. Interestingly, this conforms to the wavelength range of MWCNT dispersions [31]. Significantly in this region, the absorbance value of the inks increased as the concentration of active ingredient of the ink increased (same for MWCNT and F-MWCNT). However, the absorbance peaks of F-MWCNT inks are higher than MWCNT inks for all the concentrations investigated. This is an indication that at the same concentration, there are larger numbers of individually dispersed F-MWCNTs than MWCNTs in the formulated inks [29]. This may be attributed to the improved interaction between the GA surfactant and F-MWCNTs as discussed in Sect. 3.1, perhaps due to the presence of additional functionalities on the surface of the F-MWCNTs compared to the MWCNTs. The presence of –OH groups on the surface of F-MWCNT would create plenty surface area for the adsorption of the dispersant (GA) molecules. The increased amount of GA adsorption on the F-MWCNT surface will invariably improve the dispersion of F-MWCNT [29]. This might have contributed to the higher absorbance of F-MWCNT, probably due to presence of larger numbers of individually dispersed F-MWCNT compared to the non-functionalized MWCNT.

### 3.3 Ink viscosity

Asides good stability and excellent dispersion, another important criterion for ensuring good printability of formulated water-based inks is that the ink should have good viscosity and low surface tension. Generally, sufficient viscosity helps to generate stable drops from the nozzle during printing, and this is commonly achieved using additives. On the other hand, the surface tension of water-based inks should be reduced so that it is lower than the surface energy of the substrate. This is because too high surface tension could cause the ink droplets to remain in the nozzle of the cartridge, which is highly undesirable

[32]. In this study, propylene glycol was used as co-solvent to increase the ink viscosity, whereas triton-x 100 was used to decrease the surface tension of the ink. This in turn could help to disrupt the weak Marangoni flow, which helps to reduce the coffee-ring effect [33]. The results of ink viscosity measured by using a rheometer, for the different ink formulations are presented in Table 1. As presented in the table, it is evident that the viscosity of the inks is in the range of 1.37 to 3.97 mPa s. Significantly, the viscosity value increased with increasing concentration of MWCNT/F-MWCNT. This can be attributed to increased number of GA-induced dispersed particle, as the concentration of MWCNT/F-MWCNT increases. Shin et al. [34] have previously reported that an ideal ink for inkjet printing should have a viscosity in the range of 1–20 mPa s. Therefore, it can be inferred that the inks formulated in this study meets the viscosity requirement for inkjet printing. Nevertheless, it is worthy of note that the F-MWCNT inks exhibit higher viscosity than MWCNT inks (Table 1). This is believed to be due to the presence of additional functionalities on the F-MWCNT surface which might have facilitated better interaction of the particles with GA, thereby improving dispersion, and invariably the ink viscosity.

### 3.4 Wettability

Contact angle measurement was used to evaluate the wettability of the formulated inks, by placing drops of the ink on a PU substrate. The contact angle of the ink droplet was then measured using a goniometer. Hydrophobic or partially hydrophilic surfaces such as PU would normally repel water molecules such that a drop of liquid on their surface would not wet the surface, thereby forming a large contact angle. The contact angle of the different ink formulations is illustrated in Fig. 7 while the actual values are included in Table 1. As can be seen in Table 1; Fig. 7, the contact angle of the MWCNT and F-MWCNT

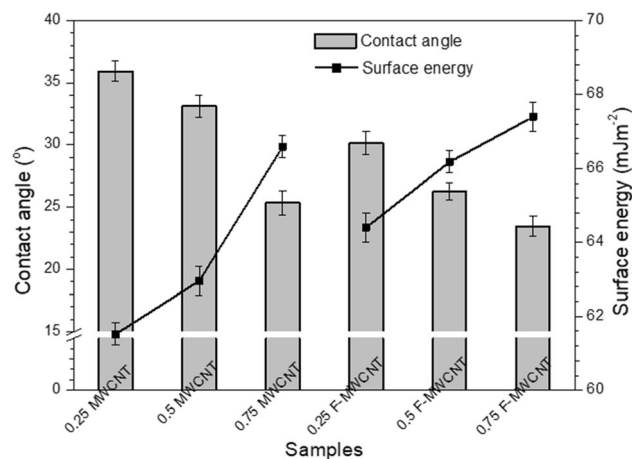


**Fig. 7** Contact angle of MWCNT and F-MWCNT inks deposited on PU substrate, and surface energy of the PU substrate during contact angle measurement

inks are significantly low ( $< 40^\circ$ ), at all the concentrations investigated. This is an indication of good wetting ability. Unlike organic solvents, water is known to possess a relatively high surface tension, because of the strong cohesive interaction between water molecules. In this study, the presence of surfactants such as GA and triton-x 100 in the formulated inks might have helped to reduce the surface tension of water as the surfactant molecules accumulate on the water-air interface due to their amphiphilic structure. This will invariably reduce the cohesive forces between the water molecules at the surface. In turn, the surface tension will become reduced such that the liquid spreads out more easily on a given surface, thereby lowering the contact angle [32].

Significantly, it can be observed from the data in Table 1 that as the concentration of the main component (MWCNT/F-MWCNT) in the ink increases, there is a subsequent decrease in contact angle. For instance, the contact angle decreased from  $35.94^\circ$  for 0.25 wt% MWCNT to  $33.12^\circ$  and  $25.36^\circ$  for 0.5 and 0.75 wt% MWCNT inks, respectively. Likewise, the

**Table 1** Viscosity and contact angle of MWCNT and F-MWCNT inks, and surface energy of the substrate during contact angle measurement

Sample	Viscosity (mPa s)	Contact angle ( $^\circ$ )	Surface energy (mJ/m <sup>2</sup> )
0.25 wt% MWCNT	1.37	35.94	61.52
0.5 wt% MWCNT	1.61	33.12	62.96
0.75 wt% MWCNT	1.92	25.36	66.59
0.25 wt% F-MWCNT	2.63	30.15	64.41
0.5 wt% F-MWCNT	2.80	26.29	66.18
0.75 wt% F-MWCNT	3.97	23.46	67.40

contact angle decreased from  $30.15^\circ$  for 0.25 wt% F-MWCNT ink to  $26.29^\circ$  and  $23.46^\circ$  for 0.5 and 0.75 wt% F-MWCNT inks, respectively. This notable decrease in contact angle as particle loading was increased is attributed to increased particle-surfactant interaction which might have increasingly reduced the cohesive forces between the water molecules. It is noticeable that the F-MWCNT inks exhibit lower contact angle which indicates better wettability. This can be possibly attributed to higher hydrophilic property of F-MWCNT which might have facilitated better dispersion in water, thereby creating more space for interaction with the surfactants. Improved interaction between the F-MWCNTs and the surfactant would invariably reduce the cohesive forces between the water molecules, thereby lowering the contact angle.

Figure 7 also shows that the surface energy of the substrate for the different ink formulations is inversely proportional to the contact angle of the ink. Specifically, at low contact angle, the surface energy is high. This is a further indication that the ink wettability and adhesion to substrate is improved as the cohesive forces are reduced and contact angle drops. Otherwise, the ink droplets could bead-up on the substrate surface. Generally, ink resistance is often due to the cohesive or intermolecular forces on its interfacial surface [35]. Therefore, the higher surface energy of the substrate would be able to break the ink resistance, thereby deforming it into a new surface [36]. Hence, it can be inferred that the formulated inks are print compatible, considering their low contact angle.

### 3.5 Electrical conductivity of printed MWCNT and F-MWCNT ink

The electrical conductivity of the printed MWCNT and F-MWCNT inks was measured at varying printed layers, using a resistance meter. Six samples were measured for each category of layers and the result of the average values are illustrated in Fig. 8. Generally, the result shows that the conductivity increases as the number of printed layers increased, both for MWCNT and F-MWCNT inks. This is attributed to increased magnitude of conducting cross-section as the number of printing layer increases. Furthermore, Fig. 8 reveals that the electrical conductivity of the samples is largely dependent on the concentration of conductive particles (MWCNTs/F-MWCNTs) in the

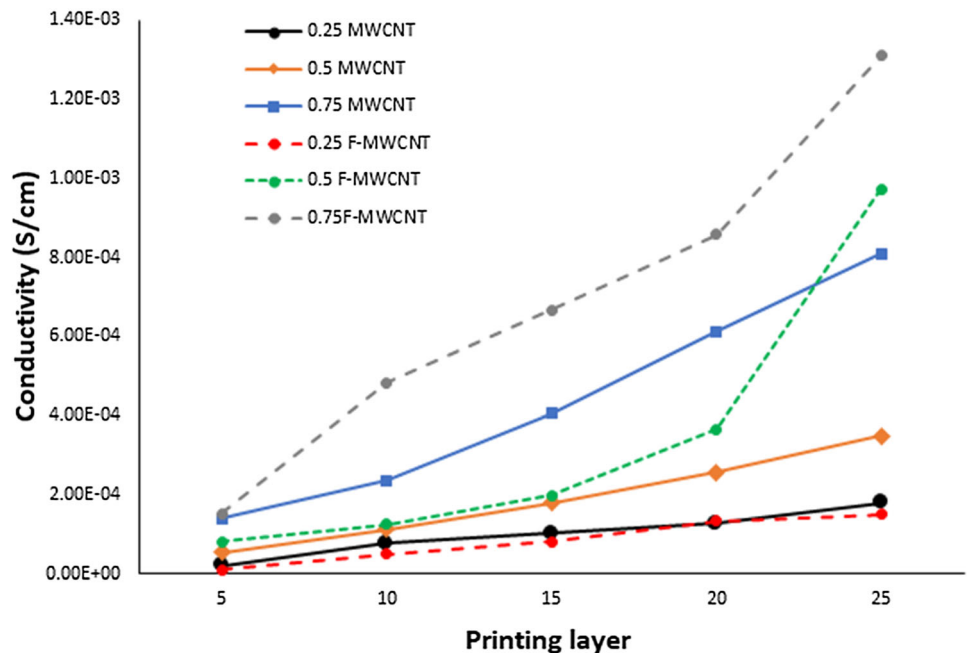
ink. Specifically, the electrical conductivity increases as the concentration of conductive particles in the ink increases, regardless of the type of conductive component, be it MWCNT or F-MWCNT. Significantly, as the number of printing layer increases, there is a more drastic increase in the electrical conductivity of the ink at 0.75 wt% concentration of conductive component. It should be noted that the concentrations investigated in this study are based on preliminary investigations. Specifically, the electrical conductivity of the ink is too low at very low concentration ( $< 0.25$  wt%). On the other hand, above 0.75 wt%, there is a drastic drop in the ink stability and dispersion. This suggests that an optimally high concentration of conductive component helps to produce sufficient thickness to facilitate improved conductivity, as the printing layer increased. This is an indication that an effective conducting network of printed MWCNTs and F-MWCNTs was generated at a sufficiently high particle concentration as reported previously [37]. Defects can be easily formed on the substrate when the number of printed layers is less. This is believed to have contributed to the low electrical conductivity of the printed inks at 5 L. However, as the number of printing layer is increased, a continuous conductive network can be formed, which is believed to have contributed to the significantly higher conductivity of the printed ink at higher printed layers, especially at 25 L. This was further investigated by observing the morphology of the printed tracks which is discussed in the subsequent section.

### 3.6 Morphological properties of printed tracks

Figure 9 shows the morphology of the MWCNT printed tracks on PU substrate. The image presented in Fig. 9a is the bird view of the printed 0.25 wt% MWCNT ink at 5 L. The image shows the boundary between the substrate and the printed ink. Specifically, the presence of MWCNTs and clusters that have been coated on the substrate is indicated on the image (Fig. 9a). In addition, nanosized pores which represent the top surface of the clean substrate is indicated on the image. Figure 9b shows the image of the same sample which has been magnified to 100 K where the presence of MWCNT network can be observed together with the defects such as holes distributed over the surface of the printed track. This



**Fig. 8** Electrical conductivity of printed MWCNT and F-MWCNT inks versus printed layer



could make it difficult for the ink at this number of printed layers to form sufficient conductive network, which is believed to have caused the low-electrical conductivity ( $2.1 \times 10^{-5}$  S/cm) of the 5 L printed 0.25 wt% MWCNT ink (Fig. 8). In contrast, at higher printed layers (25 L) as shown in Fig. 9c, the surface of the substrate was totally covered with denser MWCNT network. Nevertheless, there is no significant difference in the electrical conductivity, even at 25 L. This is perhaps due to the low concentration of MWCNTs in this formulation. Similarly, defect holes can be seen in the image of 0.75 wt% MWCNT at 5 L (Fig. 9d), which accounts for the negligible difference in electrical conductivity of 0.75 wt% MWCNT and 0.25 wt% MWCNT at 5 L (Fig. 8). However, at 25 L for 0.75 wt% MWCNT ink (Fig. 9e), the MWCNT network appears to be densely packed which produced a significantly higher electrical conductivity, perhaps due to formation of sufficient conductive path at this MWCNT concentration and printed layers. Similar observation was reported by Karim et al., for inkjet printed AgNPs conductive ink [16].

The morphology of the F-MWCNT ink (not shown) at 0.25 wt% and 0.75 wt% F-MWCNT concentrations are like the MWCNT ink shown in Fig. 9. Specifically, at fewer printing layers (5 L), pores and defects can be seen on the image whereas at higher printing layer (25 L), a more densely packed network structure can be observed for 0.25 wt% and 0.75 wt% F-MWCNT

concentrations. However, based on the result in Fig. 8, it can be seen that at 25 L, the electrical conductivity of the 0.5 wt% F-MWCNT printed ink is higher than 0.75 wt% MWCNT printed ink, despite the higher concentration of conductive component in the 0.75 wt% MWCNT ink. Therefore, it can be inferred that as the number of printing layer increases, there is higher synergy between concentration and number of printing layers in F-MWCNT printed ink to produce high electrical conductivity, compared to MWCNT printed ink. This can be attributed to the better dispersion of F-MWCNT and increased F-MWCNT-surfactant interaction in the F-MWCNT inks. This might have accelerated the generation of effective conductive tracks as the printing layer increases, by spreading more evenly on the substrate thereby closing all possible defect holes and bridging the conductive paths. This explains the significantly higher electrical conductivity of the F-MWCNT printed ink as discussed in Sect. 3.5 and illustrated in Fig. 8.

### 3.7 Stretching properties

Based on the results obtained from the previous sections, it can be inferred that F-MWCNT inks perform better than MWCNT inks, especially in terms of particle dispersion, stability, and electrical conductivity. Therefore, the electromechanical properties of the F-MWCNT ink at different F-MWCCNT

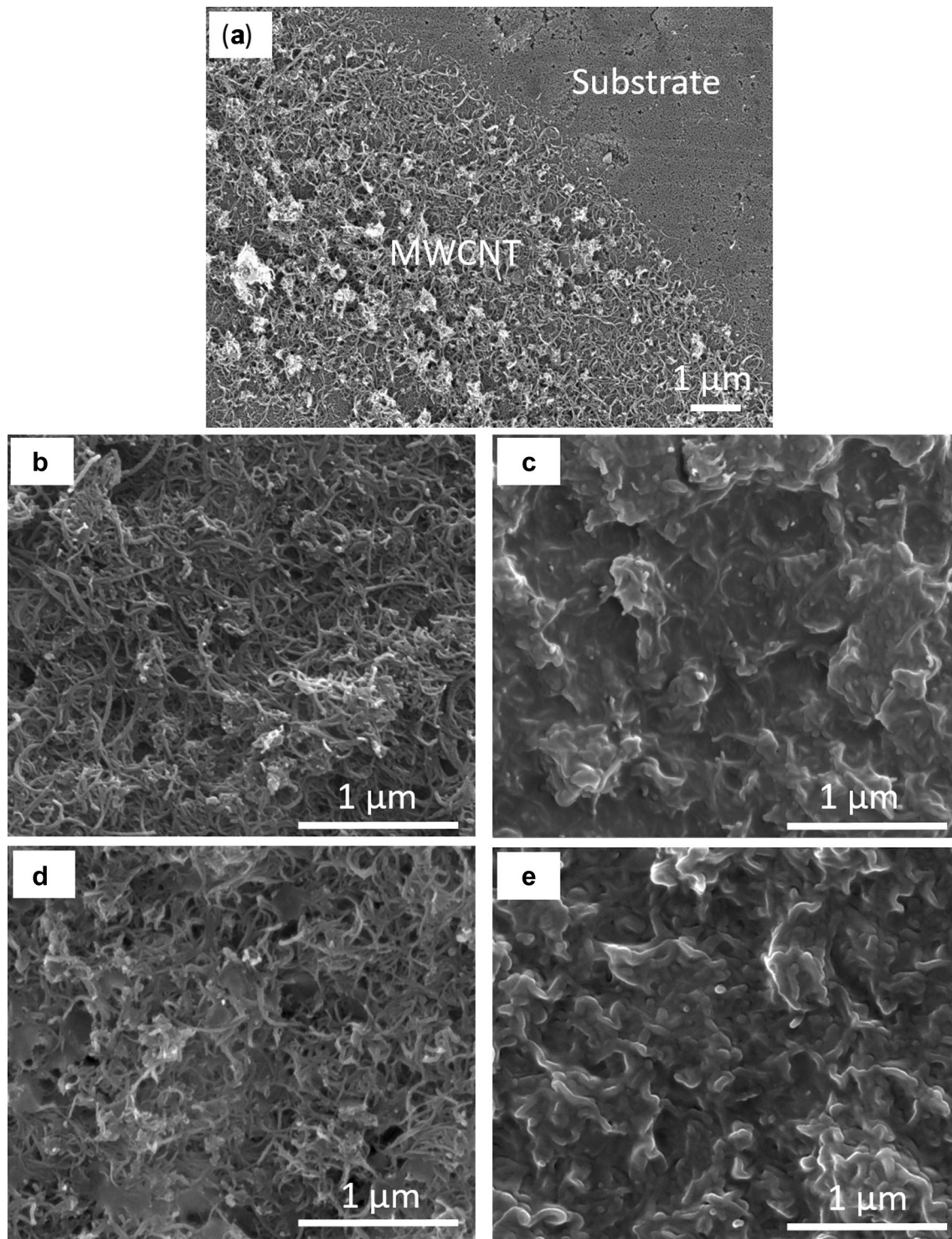


**Fig. 9** SEM images of **a** bird eye view of MWCNT conductive track on PU substrate at 5 L, **b** 0.25 wt% MWCNT conductive track on PU substrate at 5 L, **c** 0.25 wt% MWCNT conductive

track on PU substrate at 25 L, **d** 0.75 wt% MWCNT conductive track on PU substrate at 5 L, and **e** 0.75 wt% MWCNT conductive track on PU substrate at 25 L

concentration was assessed using tensile test. The resistance of the flexible substrate printed ink at different strains such as 0, 5, 10, and 20% strain is

illustrated in Fig. 10. As can be seen in the figure, the resistance trend of the printed inks at different F-MWCNT concentration is similar. Nevertheless, it

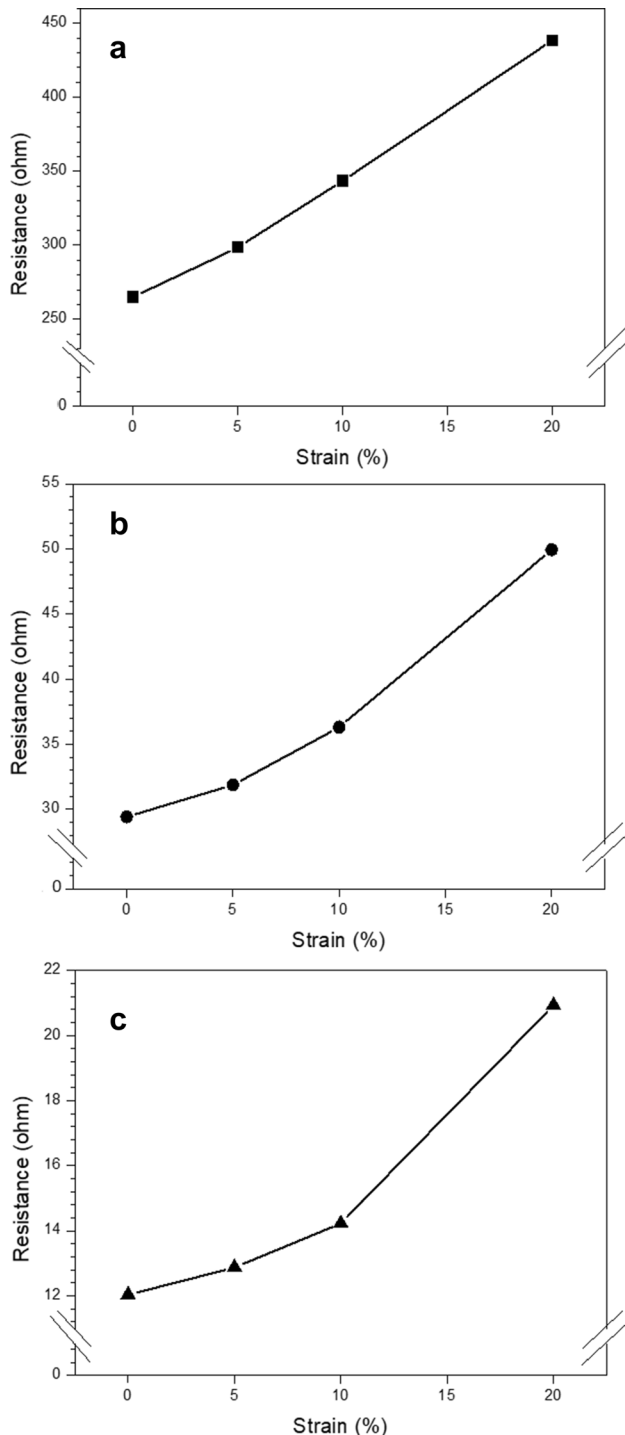


**Fig. 10** Resistance of printed F-MWCNT ink at different strain (0%, 5%, 10%, and 20%) for **a** 0.25 wt% F-MWCNT, **b** 0.5 wt% F-MWCNT, and **c** 0.75 wt% F-MWCNT concentrations

is noteworthy that as the F-MWCNT concentration increases, the resistance of the printed flexible electronic becomes reduced. Hence, printed 0.75 wt% F-MWCNT ink (Fig. 10c) exhibits the lowest

resistance at all strain levels. Generally, good linearity and reasonably low resistance values is important for flexible sensors subjected to strain [38, 39]. However, considering the result in Fig. 10, it can be concluded that at low F-MWCNT concentration, the linearity of the printed ink is poor. This is why the stretching of the low concentration printed F-MWCNT ink produced significant changes in resistance values, which is undesirable [39]. This can be associated with the poorly connected conductive tracks in the printed 0.25 wt% F-MWCNT ink, as revealed by the SEM analysis. Specifically, the presence of pore defects in the printed 0.25 wt% F-MWCNT ink might have triggered breakage of conductive network, thereby increasing the resistance (Fig. 10a). On the other hand, the densely packed structure can be obtained by printing the 0.75 wt% F-MWCNT ink, especially at higher number of printing layers. In addition, the formation of good conductive path as discussed in the previous section is believed to have contributed to relatively low change in resistance of the printed 0.75wt% F-MWCNT ink (Fig. 10c). This in turn will invariably produce low resistance of the printed ink, as seen in Fig. 10b and c.

## 4 Conclusions

A simple method for generating electrically conductive MWCNT patterns on PU is demonstrated in this study. Functionalized MWCNTs (F-MWCNTs) and non-functionalized MWCNT (MWCNT) were dispersed in water to prepare CNT dispersions, which are suitable for inkjet printing. The fluidic properties of the ink, such as viscosity, wetting, adsorption and fixation on the PU substrate were satisfactorily achieved. The ink can be successfully printed on the substrate for several passes, with the electrical conductivity reaching up to  $8.11 \times 10^{-4}$  S/cm and  $1.31 \times 10^{-3}$  S/cm after 25 passes for MWCNT and F-MWCNT printed inks, respectively. Being a simple aqueous dispersion of F-MWCNTs and MWCNTs, the ink formulation developed in this study is environmentally friendly, easy to handle and store. In addition, the ink was successfully printed using a commercial desktop inkjet printer, thereby allowing the use of inexpensive printing cartridges and substrates. Therefore, the ink shows great potential for green and mass production of CNT sensors via inkjet

printing. It is expected that with more sophisticated inkjet printer and proper optimization of the printing parameters, this approach will grow into a comparatively competitive technology for fabricating future low-cost flexible electronic devices. This will in turn contribute towards global economic growth.

## Acknowledgements

The authors would like to thank the Universiti Sains Malaysia for their contribution to this project through Fundamental Research Grant (MRSA: Grant No.: 6071385).

## Funding

The fund used for this study was provided by Universiti Sains Malaysia through Fundamental Research Grant (MRSA: Grant No.: 6071385).

## Declarations

**Conflict of interest** The authors declare no conflict of interest.

## References

- C. Cano-Raya et al., Chemistry of solid metal-based inks and pastes for printed electronics—a review. *Appl. Mater. Today* **15**, 416–430 (2019)
- A.M. Abdelkader et al., Ultraflexible and robust graphene supercapacitors printed on textiles for wearable electronics applications. *2D Mater.* **4**(3), 035016 (2017)
- L. Zhou et al., All-organic active matrix flexible display. *88*(8), 083502 (2006)
- N. Karim et al., All inkjet-printed graphene-based conductive patterns for wearable e-textile applications. *J. Mater. Chem. C* **5**(44), 11640–11648 (2017)
- M.V. Kulkarni et al., Ink-jet printed conducting polyaniline based flexible humidity sensor. *Sens. Actuators B* **178**, 140–143 (2013)
- N. Matsuhisa et al., Printable elastic conductors by in situ formation of silver nanoparticles from silver flakes. *Nat. Mater.* **16**(8), 834–840 (2017)
- M. Jung et al., All-printed and roll-to-roll-printable 13.56-MHz-operated 1-bit RF tag on plastic foils. *IEEE Trans. Electron Devices* **57**(3), 571–580 (2010)
- A. Chauraya et al., Inkjet printed dipole antennas on textiles for wearable communications. *IET Microw. Antennas Propag.* **7**, 760–767 (2013)
- G.H. Gelinck et al., Flexible active-matrix displays and shift registers based on solution-processed organic transistors. *Nat. Mater.* **3**(2), 106–110 (2004)
- N. Matsuhisa et al., Printable elastic conductors with a high conductivity for electronic textile applications. *Nat. Commun.* **6**(1), 7461 (2015)
- H. Menon, R. Aiswarya, K.P. Surendran, Screen printable MWCNT inks for printed electronics. *RSC Adv.* **7**(70), 44076–44081 (2017)
- D.J. Finn, M. Lotya, J.N. Coleman, Inkjet printing of silver nanowire networks. *ACS Appl. Mater. Interfaces* **7**(17), 9254–9261 (2015)
- E.B. Secor et al., Gravure printing of graphene for large-area flexible electronics. *Adv. Mater.* **26**(26), 4533–4538 (2014)
- M.F.L. De Volder et al., Carbon nanotubes: present and future commercial applications. *Science* **339**(6119), 535–539 (2013)
- S. Azoubel, S. Shemesh, S. Magdassi, Flexible electroluminescent device with inkjet-printed carbon nanotube electrodes. *Nanotechnology* **23**(34), 344003 (2012)
- N. Karim et al., All Inkjet-printed graphene-silver composite ink on textiles for highly conductive wearable electronics applications. *Sci. Rep.* **9**(1), 8035 (2019)
- E.B. Secor et al., Inkjet printing of high conductivity, flexible graphene patterns. *J. Phys. Chem. Lett.* **4**(8), 1347–1351 (2013)
- M.N. Karim et al., Towards UV-curable inkjet printing of biodegradable poly (lactic acid) fabrics. *J. Mater. Sci.* **50**(13), 4576–4585 (2015)
- S. Kholghi Eshkalak et al., A review on inkjet printing of CNT composites for smart applications. *Appl. Mater. Today* **9**, 372–386 (2017)
- F. Loghin et al., A facile and efficient protocol for preparing residual-free single-walled carbon nanotube films for stable sensing applications. *Nanomaterials* **9**(3), 471 (2019)
- A.N. Omrani et al., Effects of multi walled carbon nanotubes shape and size on thermal conductivity and viscosity of nanofluids. *Diam. Relat. Mater.* **93**, 96–104 (2019)
- L. Chen et al., Rheological behaviors of nanofluids containing multi-walled carbon nanotube. *J. Dispersion Sci. Technol.* **32**(4), 550–554 (2011)
- L. Maillaud et al., Effect of the rheological properties of carbon nanotube dispersions on the processing and properties of transparent conductive electrodes. *Langmuir* **31**(21), 5928–5934 (2015)
- E. Patrice et al., Shear history effect on the viscosity of carbon nanotubes water-based nanofluid. *Curr. Nanosci.* **9**(2), 225–230 (2013)

25. N.H. Ismail, J.O. Akindoyo, M. Mariatti, Solvent mediated dispersion of carbon nanotubes for glass fibre surface modification—suspensions stability and its effects on mechanical, interlaminar and dynamic mechanical properties of modified glass fibre reinforced epoxy laminates. *Compos. Part A: Appl. Sci. Manuf.* **139**, 106091 (2020)
26. Z. Xu et al., Efficient dispersion of carbon nanotube by synergistic effects of sisal cellulose nano-fiber and graphene oxide. *Compos. Interfaces* **24**(3), 291–305 (2017)
27. Y. Liu et al., Aqueous dispersion of carbon fibers and expanded graphite stabilized from the addition of cellulose nanocrystals to produce highly conductive cellulose composites. *ACS Sustain. Chem. Eng.* **6**(3), 3291–3298 (2018)
28. T.S. Tran, N.K. Dutta, N.R. Choudhury, Graphene inks for printed flexible electronics: graphene dispersions, ink formulations, printing techniques and applications. *Adv. Coll. Interface. Sci.* **261**, 41–61 (2018)
29. J. Hou et al., Effective dispersion of multi-walled carbon nanotubes in aqueous solution using an ionic-gemini dispersant. *J. Colloid Interface Sci.* **512**, 750–757 (2018)
30. L. Lin, H. Peng, G. Ding, Dispersion stability of multi-walled carbon nanotubes in refrigerant with addition of surfactant. *Appl. Therm. Eng.* **91**, 163–171 (2015)
31. L. Yue et al., Epoxy composites with carbon nanotubes and graphene nanoplatelets—dispersion and synergy effects. *Carbon* **78**, 268–278 (2014)
32. R.P. Tortorich, J.-W. Choi, Inkjet printing of carbon nanotubes. *Nanomaterials* **3**(3), 453–468 (2013)
33. D. McManus et al., Water-based and biocompatible 2D crystal inks for all-inkjet-printed heterostructures. *Nat. Nanotechnol.* **12**(4), 343–350 (2017)
34. K.-Y. Shin, J.-Y. Hong, J. Jang, Micropatterning of graphene sheets by inkjet printing and its Wideband Dipole-Antenna Application. *Adv. Mater.* **23**(18), 2113–2118 (2011)
35. J.N. Israelachvili, *Intermolecular and Surface Forces* (Academic press, Cambridge, 2011).
36. V.S. Turkani et al., A highly sensitive printed humidity sensor based on a functionalized MWCNT/HEC composite for flexible electronics application. *Nanoscale Adv.* **1**(6), 2311–2322 (2019)
37. O.-S. Kwon et al., Fabrication and characterization of inkjet-printed carbon nanotube electrode patterns on paper. *Carbon* **58**, 116–127 (2013)
38. S. Shengbo et al., Highly sensitive wearable strain sensor based on silver nanowires and nanoparticles. *Nanotechnology* **29**(25), 255202 (2018)
39. Y.Z.N. Htwe, I.N. Hidayah, M. Mariatti, Performance of inkjet-printed strain sensor based on graphene/silver nanoparticles hybrid conductive inks on polyvinyl alcohol substrate. *J. Mater. Sci.: Mater. Electron.* **31**(18), 15361–15371 (2020)

**Publisher's note** Springer Nature remains neutral with regard to jurisdictional claims in published maps and institutional affiliations.